Influence of taxol and CNTs on the stability analysis of protein microtubules

E. Rohani Rad [a],* and M.R. Farajpour [b]

[a] Faculty of Health and Medical Sciences, Adelaide Medical School, University of Adelaide, Adelaide, Australia
[b] Borjavaran Center of Applied Science and Technology, University of Applied Science and Technology, Tehran, Iran

---

ARTICLE INFO

ABSTRACT

Microtubules are used as targets for anticancer drugs due to their crucial role in the process of mitosis. Recent studies show that carbon nanotubes (CNTs) can be classified as microtubule-stabilizing agents as they interact with protein microtubules (MTs), leading to interference in the mitosis process. CNTs hold a substantial promising application in cancer therapy in conjunction with other cancer treatments such as radiotherapy and chemotherapy. In the current study, a size-dependent model is developed for the stability analysis of CNT-stabilized microtubules under radial and axial loads. A nonlocal shell theory with strain gradient effects is employed to take size influences into account. Moreover, Van der Waals interactions between CNTs and MTs are simulated. An excellent agreement is observed between the present model and reported data from experiments on protein MTs. In addition, the effects of taxol, as another stabilizing agent, on the stability of microtubules are studied. It is found that both nonlocal and strain gradient effects are essential to accurately obtain the stability capacity of MTs. Furthermore, CNTs have an increasing effect on the critical loads of microtubules while the critical loads reduce in the presence of taxol.

---

1. Introduction

Carbon nanotubes (CNTs) are a significant class of nanoscale structures since they exhibit excellent physical and mechanical properties. CNTs have many promising applications in health and medical sciences [1]. CNTs can be applied in conjunction with traditional drugs in order to improve available treatments. For instance, single-walled CNTs conjugated to antibodies have shown the potential to be used for targeting intestinal cancer cells [2, 3]. Furthermore, CNTs have been employed as nanoscale carriers to deliver different kinds of therapeutic molecules [4]. Moreover, Bardhan et al. [5] utilised CNTs as bacterial probes by using fluorescence imaging in order to screen pathogenic infections. In another study [6], a CNT-based biosensor was fabricated to detect a very important prostate cancer biomarker (i.e. osteopontin). García-Hevia et al. [7] have observed that CNTs could penetrate into cell membrane and then cause interruption in cell division; they concluded that CNTs have the potential to be used as anticancer drugs. In other words, when CNTs penetrate into the cell, they interact with protein microtubules (MTs), resulting in mitotic arrest and then cell death [8].

There are three kinds of filaments in the cytoskeleton of a typical eukaryotic cell: 1) microtubules, 2) microfilaments and 3) intermediate filaments. MTs have an important role in maintaining the cell shape since their mechanical strength is much higher than microfilaments and intermediate filaments [9]. Furthermore, they provide a platform for protein transport inside the cell [10]. Protein MTs also form mitotic spindles, which are essential fundamental structures in chromosome segregation during the cell division [11]. MTs are made of parallel protofilaments, which are placed in the form of a hollow cylinder. In each protofilament, α- and β-tubulin heterodimers are arranged in a head-to-tail configuration to form the structure [12].

Improving the of knowledge of the mechanics of protein MTs would be useful for better simulating the mechanical behavior of the entire cell since MTs are the most rigid filaments and bear the majority of external loads [9]. Cell mechanics [13] holds a substantial promise to be used in medical science for enhancing diagnosis techniques and screening the efficiency of medicines. For instance, it has been reported that the mechanical properties of cancer cells are noticeably different from those of healthy ones; this difference can be used for early cancer diagnosis purposes [14]. There are several experimental techniques such as the thermal fluctuation [15] and optical tweezers [16] for obtaining the mechanical properties of MTs. In addition, theoretical approaches have recently been introduced for analysing the mechanics of protein MTs. Especially, size-dependent models for these ultrasmall biological structure have been developed [17] along with the development of size-dependent models for CNTs [18, 19], nanorods [20, 21], nanobeams [22-26] and nanoplates [27-31]. A classical shell model [32], a constitutive relation [33] and a classical beam model [34] have been developed for determining the mechanical behavior of MTs; size effects are neglected in these research

---

studies. Size effects on the mechanics of MTs are important as the average diameter of these structures is about several nanometers. A number of size-dependent models have been introduced in the literature for MTs using the strain gradient elasticity [35], Pasternak model [36], surface elasticity theory [37] and modified couple stress theory [38] as well as nonlocal finite element method [39].

Since MTs have a significant role in the mitosis, they can be applied as targets for antineoplastic drugs [40]. There are two kinds of anticancer drugs that target MTs: 1) microtubule-stabilizing drugs and 2) microtubule-destabilizing drugs. The stabilizing agents such as taxol and epothylone lead to the polymerisation of tubulin dimers into microtubules, while destabilizing drugs such as colchicine and vinblastine depolymerise MTs. Both kinds of drugs prevent chromosomes from normal arrangement at metaphase and interfere with forming the mitotic spindle, arresting cells in metaphase. This leads to the activation of a mechanism that monitors the correct chromosome segregation termed spindle assembly checkpoint (SAC) [40]. Protracted activation of the SAC prevents anaphase onset and finally causes cell death. Recent groundbreaking studies have shown that CNTs behave as MT-stabilizing agents and could be used in future cancer therapies in combination with traditional chemotherapeutic agents [7]. Thus, understanding the interaction between CNTs and MTs is an important problem.

In this study, a size-dependent shell model is developed for the static stability analysis of protein MTs stabilised with taxol and CNT. Size effects are considered via a continuum model incorporating two scale parameters. The influences of nonlocal mechanical stress, strain gradients and orthotropic elastic properties are captured. Furthermore, van der Waals (vdW) interactions between MTs and CNTs are also incorporated. The hybrid nanostructure is subjected to both radial pressure and axial force. For comparison purposes, the experimental results from the literature on MTs are used, and the proposed model is verified. Numerical results are determined for three types of stabilising factors: 1) microtubule-associated proteins (MAPs), and 2) CNTs 3) taxol. Finally, size effects on the stability of MTs stabilized with MAPs, taxol and CNTs are studied. To suitably design future generations of chemotherapeutic agents using carbon nanotubes, the presented model could be useful.

2. Methods

2.1. A nonlocal strain gradient model

The application of the classical nonlocal models is restricted because they can only capture stiffness softening in the mechanical behavior at nanoscales. Nonetheless, lastly, a powerful size-dependent theory, which is able to capture both stiffness softening and hardening, has been introduced [41-43]. The influences of the nonlocality in stress and strain components are incorporated in this theory by employing two distinct scale parameters [41]. The basic equation of the theory (i.e. nonlocal strain gradient) is written as [41]

$$\boldsymbol{\sigma} = \iiint_V \psi_0 \left[\chi_0, |\mathbf{x}' - \mathbf{x}| \right] (\mathbf{C}:\boldsymbol{\varepsilon}) dV \;,$$

$$\boldsymbol{\sigma}^{(1)} = \ell_s^2 \iiint_V \psi_1 \left[\chi_1, |\mathbf{x}' - \mathbf{x}| \right] (\mathbf{C}:\nabla\boldsymbol{\varepsilon}) dV \;, \qquad (1a,b)$$

in which ":" indicates the double-dot product; $\boldsymbol{\sigma}$ and $\boldsymbol{\sigma}^{(1)}$ represent the lower-order and first-order nonlocal stresses, respectively; $\mathbf{C}$, $\boldsymbol{\varepsilon}$ and V indicate elasticity tensor, strain and microtubule volume, respectively; also, ∇ is the gradient

operator; ℓ_s, ψ_0 and ψ_1 stand for the strain gradient parameter, nonlocal lower-order and first-order attenuation functions, respectively; $|\mathbf{x}' - \mathbf{x}|$ is the distance from $\mathbf{x}$ to $\mathbf{x}'$ [44-47]; the lower-order and first-order scale coefficients associated with stress nonlocality are denoted by χ_0 and χ_1, respectively [48-51]. The definition of these coefficients are, respectively, as $\chi_0 = e_0 a/L$ and $\chi_1 = e_1 a/L$ in which a, L and $e_i (i = 0,1)$ are an internal characteristic length of the MT (as an illustration the length of the tubulin dimer) [52-55], the length of the MT and calibration constants, respectively. The stress components are related as

$$\boldsymbol{\sigma}^t = \boldsymbol{\sigma} - \nabla \cdot \boldsymbol{\sigma}^{(1)} \qquad (2)$$

On the other hand, for the nonlocal attenuation functions, we have

$$\lim_{\chi_0 \to 0} \psi_0 \left[\chi_0, |\mathbf{x} - \mathbf{x}'| \right] = \delta \left(|\mathbf{x} - \mathbf{x}'| \right),$$

$$\lim_{\chi_1 \to 0} \psi_1 \left[\chi_1, |\mathbf{x} - \mathbf{x}'| \right] = \delta \left(|\mathbf{x} - \mathbf{x}'| \right). \qquad (3a,b)$$

Here δ is the Dirac delta function. Since the implementation of Eq. (1) in the size-dependent modelling of protein MTs is difficult, the following differential equation is recommended [41, 56]

$$\sigma_{ij}^t - (e_0 a)^2 \nabla^2 \sigma_{ij}^t = C_{ijkl} \varepsilon_{kl} - C_{ijkl} \ell_s^2 \nabla^2 \varepsilon_{kl}. \qquad (4)$$

It should be noticed that the two calibration parameters are assumed to be the same ($e_0 = e_1$) for the sake of simplification. In Eq. (4), ∇^2 is the Laplacian operator. Lately, a nonlocal strain gradient model of beams has successfully been used by Li et al. [43] to explore the size-dependent mechanics of CNTs; it has been proven that nonlocal strain gradient models are more reliable compared to their classical nonlocal counterparts.

2.2. A shell model for CNT-stabilized MTs

Carbon nanotubes and protein microtubules are both hollow nanotubes and are of similar dimensions (Figs.1 and 2). Recently, it has been demonstrated that interaction between CNTs and MTs inside human cancer cells (HeLa) blocks mitosis and causes cell death by apoptosis [7] (Fig. 3). Therefore, CNTs have similar effects as spindle poisons such as taxol, vinca alkaloids or epothilones. Carbon nanotubes can be used as a promising synthetic MT-stabilizing agent for future chemotherapeutic trials. There are two models for CNT-MT interaction: 1) carbon nanotube-microtubule mixed bundles and 2) biomimetic microtubules [8]. In the CNT-MT mixed bundle, CNTs longitudinally interact with MTs and limit their dynamic behaviour. In the biomimetic MT model, at least one protofilament of the MT is replaced by nanotubes. The biomimetic microtubule model occurs in the case in which the nanotube diameter is close to that of protofilaments (approximately 5 nm).
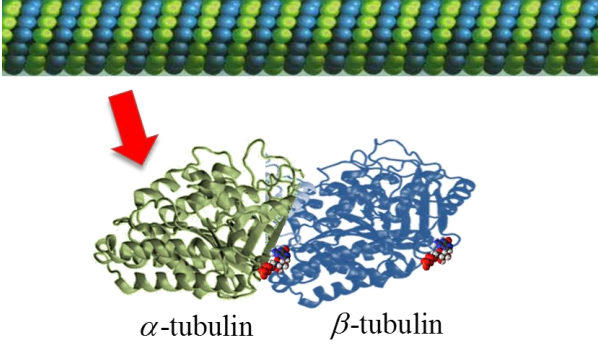
Fig. 1. The schematic representation of a protein microtubule.
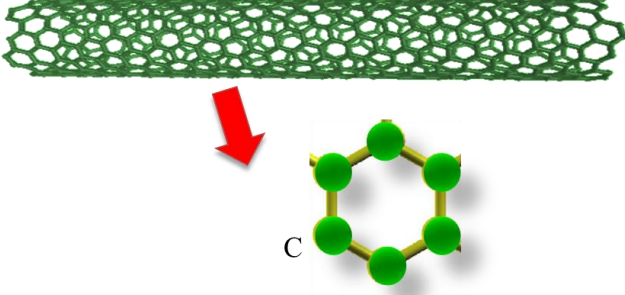
Fig. 2. The schematic representation of a single-walled carbon nanotube.
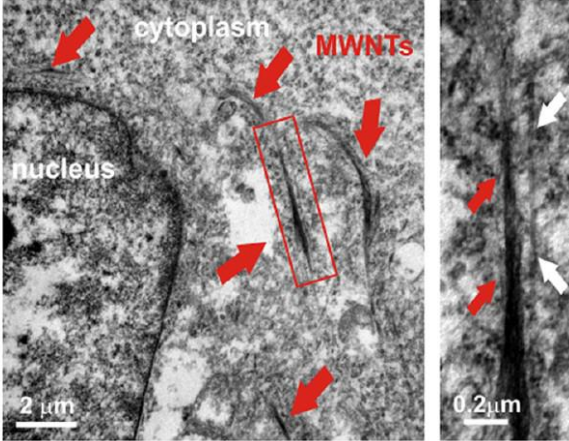
Fig. 3. The cytoplasm of HeLa cells with multi-walled carbon nanotubes (MWCNTs); white arrows indicate protein MTs while red ones indicate MWCNTs [8]; reproduced with permission from ACS Publications.

For simplification and without losing generality, it is assumed that the interaction between microtubules and carbon nanotubes is of model 1. The internal and external radii of the MT, and the radius of the CNT are denoted by R_i, R_o and R_c, respectively. In general, it is assumed that the carbon nanotube-microtubule system with length L is subjected to axial compression and external pressure. Let us denote the prestresses in axial and circumferential directions by $\hat{N}_{xx}$ and $\hat{N}_{\theta\theta}$, respectively. In addition, the external tractions that act on the MT and CNT are denoted by $f_i^{\,m}$ and $f_i^{\,c}$ ($i = x, \theta, r$), respectively. Using the general constitutive equation (4), the governing equations of the MT are obtained as follows:

$$
\left(1-\mu_s\nabla_m^2\right)\left[R_m^2 A_x^m \frac{\partial^2 u_m}{\partial x^2}+\left(A_{x\theta}^m+\frac{D_{x\theta}^m}{R_m^2}\right)\frac{\partial^2 u_m}{\partial\theta^2}\right.
$$

$$
+R_m\left(v_\theta^m A_x^m+A_{x\theta}^m\right)\frac{\partial^2 v_m}{\partial x\,\partial\theta}
$$

$$
\left.-R_m v_\theta^m A_x^m \frac{\partial w_m}{\partial x}+R_m D_x^m \frac{\partial^3 w_m}{\partial x^3}-\frac{D_{x\theta}^m}{R_m}\frac{\partial^3 w_m}{\partial x\,\partial\theta^2}\right]
$$

$$
+\left(1-\mu_0\nabla_m^2\right)\left(R_m^2 \hat{N}_{xx}\frac{\partial^2 u_m}{\partial x^2}\right.
$$

$$
+\hat{N}_{\theta\theta}\frac{\partial^2 u_m}{\partial\theta^2}+R_m\hat{N}_{\theta\theta}\frac{\partial w_m}{\partial x}+R_m^2 f_x^{\,m}\right)=0,
$$

$$
\left(1-\mu_s\nabla_m^2\right)\left[R_m\left(v_x^m A_\theta^m+A_{x\theta}^m\right)\frac{\partial^2 u_m}{\partial x\,\partial\theta}+\left(R_m^2 A_{x\theta}^m+3D_{x\theta}^m\right)\frac{\partial^2 v_m}{\partial x^2}\right.
$$

$$
\left.+A_\theta^m \frac{\partial^2 v_m}{\partial\theta^2}-A_\theta^m \frac{\partial w_m}{\partial\theta}+\left(v_x^m D_\theta^m+3D_{x\theta}^m\right)\frac{\partial^3 w_m}{\partial x^2\partial\theta}\right]+
$$

$$
\left(1-\mu_0\nabla_m^2\right)\left(R_m^2\hat{N}_{xx}\frac{\partial^2 v_m}{\partial x^2}+\hat{N}_{\theta\theta}\frac{\partial^2 v_m}{\partial\theta^2}-\hat{N}_{\theta\theta}\frac{\partial w_m}{\partial\theta}+R_m^2 f_\theta^{\,m}\right)=0,
$$

$$
\left(1-\mu_s\nabla_m^2\right)\left[R_m v_x^m A_\theta^m \frac{\partial u_m}{\partial x}-R_m D_x^m \frac{\partial^3 u_m}{\partial x^3}+\frac{D_{x\theta}^m}{R_m}\frac{\partial^3 u_m}{\partial x\,\partial\theta^2}\right.
$$

$$
+A_\theta^m \frac{\partial v_m}{\partial\theta}-\left(v_\theta^m D_x^m+3D_{x\theta}^m\right)\frac{\partial^3 v_m}{\partial x^2\partial\theta}
$$

$$
-R_m^2 D_x^m \frac{\partial^4 w_m}{\partial x^4}-2\left(v_\theta^m D_x^m+2D_{x\theta}^m\right)\frac{\partial^4 w_m}{\partial x^2\partial\theta^2}
$$

$$
\left.-\frac{D_\theta^m}{R_m^2}\left(\frac{\partial^4 w_m}{\partial\theta^4}+2\frac{\partial^2 w_m}{\partial\theta^2}+w_m\right)-A_\theta^m w_m\right]
$$

$$
+\left(1-\mu_0\nabla_m^2\right)\left(-R_m\hat{N}_{\theta\theta}\frac{\partial u_m}{\partial x}\right.
$$

$$
+\hat{N}_{\theta\theta}\frac{\partial v_m}{\partial\theta}+R_m^2\hat{N}_{xx}\frac{\partial^2 w_m}{\partial x^2}+\hat{N}_{\theta\theta}\frac{\partial^2 w_m}{\partial\theta^2}+R_m^2 f_r^{\,m}\right)=0 \quad (5a-c)
$$

Similarly, for the CNT, we have

$$
\left(1-\mu_s\nabla_c^2\right)\left[R_c^2\frac{\partial^2 u_c}{\partial x^2}+\frac{1}{2}\left(1-v_c\right)\left(1+\frac{D_c}{A_c R_c^2}\right)\frac{\partial^2 u_c}{\partial\theta^2}\right.
$$

$$
+\frac{R_c}{2}\left(1+v_c\right)\frac{\partial^2 v_c}{\partial x\,\partial\theta}-R_c v_c\frac{\partial w_c}{\partial x}
$$

$$
\left.+R_c\frac{D_c}{A_c}\frac{\partial^3 w_c}{\partial x^3}-\frac{1}{2}\left(1-v_c\right)\frac{D_c}{A_c R_c}\frac{\partial^3 w_c}{\partial x\,\partial\theta^2}\right]+\frac{1}{A_c}\left(1-\mu_0\nabla_c^2\right)
$$

$$
\times\left(R_c^2\hat{N}_{xx}\frac{\partial^2 u_c}{\partial x^2}+\hat{N}_{\theta\theta}\frac{\partial^2 u_c}{\partial\theta^2}+R_c\hat{N}_{\theta\theta}\frac{\partial w_c}{\partial x}+R_c^2 f_x^{\,c}\right)=0,
$$

$$
\left(1-\mu_s\nabla_c^2\right)\left[\frac{R_c}{2}\left(1+v_c\right)\frac{\partial^2 u_c}{\partial x\,\partial\theta}+\frac{R_c^2}{2}\left(1-v_c\right)\left(1+3\frac{D_c}{A_c R_c^2}\right)\frac{\partial^2 v_c}{\partial x^2}\right.
$$

$$
\left.+\frac{\partial^2 v_c}{\partial\theta^2}-\frac{\partial w_c}{\partial\theta}+\frac{1}{2}\left(3-v_c\right)\frac{D_c}{A_c}\frac{\partial^3 w_c}{\partial x^2\partial\theta}\right]+
$$

$$
\frac{1}{A_c}\left(1-\mu_0\nabla_c^2\right)\left(R_c^2\hat{N}_{xx}\frac{\partial^2 v_c}{\partial x^2}+\hat{N}_{\theta\theta}\frac{\partial^2 v_c}{\partial\theta^2}-\hat{N}_{\theta\theta}\frac{\partial w_c}{\partial\theta}+R_c^2 f_\theta^{\,c}\right)=0,
$$

$$
\left(1-\mu_s\nabla_c^2\right)\left[R_c v_c\frac{\partial u_c}{\partial x}-\frac{R_c D_c}{A_c}\frac{\partial^3 u_c}{\partial x^3}+\frac{1}{2}\left(1-v_c\right)\frac{D_c}{A_c R_c}\frac{\partial^3 u_c}{\partial x\,\partial\theta^2}+\frac{\partial v_c}{\partial\theta}\right.
$$

$$-\frac{1}{2}(3-\nu_c)\frac{D_c}{A_c}\frac{\partial^3 v_c}{\partial x^2 \partial \theta}-R_c^2\frac{D_c}{A_c}\frac{\partial^4 w_c}{\partial x^4}-2\frac{D_c}{A_c}\frac{\partial^4 w_c}{\partial x^2 \partial \theta^2}-\frac{D_c}{A_c R_c^2}$$

$$\times\left(\frac{\partial^4 w_c}{\partial \theta^4}+2\frac{\partial^2 w_c}{\partial \theta^2}+w_c\right)-w_c\Bigg]+\frac{1}{A_c}\left(1-\mu_0\nabla_c^2\right)\left(-R_c\hat{N}_{\theta\theta}\frac{\partial u_c}{\partial x}\right.$$

$$\left.+\hat{N}_{\theta\theta}\frac{\partial v_c}{\partial \theta}+R_c^2\hat{N}_{xx}\frac{\partial^2 w_c}{\partial x^2}+\hat{N}_{\theta\theta}\frac{\partial^2 w_c}{\partial \theta^2}+R_c^2 f_r^c\right)=0 \qquad (6a-c)$$

in which $\mu_0=(e_0 a)^2$ and $\mu_s=\ell_s^2$; the indices "*m*" and "*c*" denote the microtubule and carbon nanotube, respectively; u_i, v_i and w_i ($i=m,c$) are the components of the displacement along the axial, circumferential and radial directions, respectively. In the above equations, the Laplacian operator is given by $\nabla_i^2(\bullet)=\partial^2(\bullet)/\partial x^2+(1/R_i^2)\partial^2(\bullet)/\partial \theta^2$ for $i=m,c$. A_x^m, A_θ^m and $A_{x\theta}^m$ are the in-plane longitudinal, circumferential and shear stiffnesses of the MT, respectively. Also, D_x^m and D_θ^m are, respectively, the effective flexural rigidities of the MT in axial and circumferential axes, and $D_{x\theta}^m$ is the flexural rigidity in shear. A_c and D_c are the in-plane stiffness and flexural rigidity of the CNT, respectively. It should be noted that the governing differential equations (5) and (6) reduce to those of the classical (local) shell theory when both nonlocal and strain gradient parameters are set to zero. The in-plane and bending stiffnesses of the components of the system are defined as

$$A_x^m=\frac{E_x^m h_m}{1-\nu_x^m \nu_\theta^m}, \quad A_\theta^m=\frac{E_\theta^m h_m}{1-\nu_x^m \nu_\theta^m},$$

$$A_{x\theta}^m=G_{x\theta}^m h_m, \quad D_x^m=\frac{E_x^m h_{0m}^3}{12\left(1-\nu_x^m \nu_\theta^m\right)},$$

$$D_\theta^m=\frac{E_\theta^m h_{0m}^3}{12\left(1-\nu_x^m \nu_\theta^m\right)}, \quad D_{x\theta}^m=\frac{G_{x\theta}^m h_{0m}^3}{12},$$

$$A_c=\frac{E_c h_c}{1-\nu_c^2}, \quad D_c=\frac{E_c h_c^3}{12\left(1-\nu_c^2\right)}$$

$$(7)$$

where E_x^m, E_θ^m and $G_{x\theta}^m$ are, respectively, the MT longitudinal, circumferential and shear moduli; $\nu_i^m (i=x,\theta)$, h_m and h_{0m} are Poisson's ratios, equivalent and effective thicknesses, respectively; also, E_c, ν_c and h_c, respectively, represent elasticity modulus, Poisson's ratio and thickness of CNTs. According to the experimental data on single-walled carbon nanotubes [18], their bending rigidity is considerably lower than that of Eq. (7). Therefore, the bending rigidity of CNTs should be regarded as an independent material property. A similar behavior has been found for microtubules and thus their bending stiffness is calculated using h_{0m} whereas their in-plane stiffness is determined via h_m [36, 57]. The axial and circumferential tractions are set to zero. The radial load due to the vdW interaction is expressed as

$$f_r^c=-c_{vdW}^c\left(w_c-w_m\right), \quad f_r^m=-c_{vdW}^m\left(w_m-w_c\right) \qquad (8a,b)$$

where $c_{vdW}^j (j=m,c)$ represents the vdW interaction coefficient. All ends are simply supported. In order to satisfy these boundary conditions, the displacement components of the hybrid nanostructure can be written as

$$\begin{Bmatrix} u_c \\ v_c \\ w_c \end{Bmatrix}=\begin{Bmatrix} U_c \cos(n_\theta\theta)\cos(\alpha_x x) \\ V_c \sin(n_\theta\theta)\sin(\alpha_x x) \\ W_c \sin(\alpha_x x)\cos(n_\theta\theta) \end{Bmatrix},$$

$$\begin{Bmatrix} u_m \\ v_m \\ w_m \end{Bmatrix}=\begin{Bmatrix} U_m \cos(\alpha_x x)\cos(n_\theta\theta) \\ V_m \sin(\alpha_x x)\sin(n_\theta\theta) \\ W_m \sin(\alpha_x x)\cos(n_\theta\theta) \end{Bmatrix}, \qquad (9a-f)$$

in which $\alpha_x=n_x\pi/L$; n_x and n_θ stand for the half axial wave number and circumferential wave number, respectively. In addition, U_j, V_j and W_j ($j=m,c$) are constants related to the buckling mode shape of the system. For convenience and without losing generality, the following non-dimensional parameters are introduced

$$\bar{\alpha}_{xc}=\alpha_x R_c, \quad \chi_{0c}^2=\frac{\mu_0}{R_c^2}, \quad \chi_{sc}^2=\frac{\mu_s}{R_c^2}, \quad \bar{D}_c=\frac{D_c}{A_c R_c^2},$$

$$r_{A_x}=\frac{A_x^m}{A_c}, \quad \bar{c}_{vdW}^c=\frac{c_{vdW}^c R_c^2}{A_c},$$

$$\bar{\alpha}_{xm}=\alpha_x R_m, \quad \chi_{0m}^2=\frac{\mu_0}{R_m^2}, \quad \chi_{sm}^2=\frac{\mu_s}{R_m^2},$$

$$\bar{c}_{vdW}^m=\frac{c_{vdW}^m R_m^2}{A_x^m}, \quad \bar{N}_{xx}=\frac{\hat{N}_{xx}}{A_x^m}, \quad \bar{N}_{\theta\theta}=\frac{\hat{N}_{\theta\theta}}{A_x^m},$$

$$\bar{A}_\theta^m=\frac{A_\theta^m}{A_x^m}, \quad \bar{A}_{x\theta}^m=\frac{A_{x\theta}^m}{A_x^m}, \quad \bar{D}_x^m=\frac{D_x^m}{A_x^m R_m^2},$$

$$\bar{D}_\theta^m=\frac{D_\theta^m}{A_x^m R_m^2}, \quad \bar{D}_{x\theta}^m=\frac{D_{x\theta}^m}{A_x^m R_m^2} \qquad (10)$$

Let us first consider the axial instability of the hybrid nanostructure. In this case, the external pressure exerted on the CNT-stabilized microtubule is zero, and thus the circumferential prestress is set to zero ($\bar{N}_{\theta\theta}=0$). Substituting Eq. (9) into Eqs. (5) and (6) and using the definitions of dimensionless parameters given by Eq. (10), one can obtain

$$\left(\left[K_{ij}^{(1)}\right]-\bar{N}_{xx}\left[K_{ij}^{(2)}\right]\right)\{U\}=0, \qquad (11)$$

Similarly, for the radial instability of CNT-stabilized microtubules ($\bar{N}_{xx}=0$), we have

$$\left(\left[K_{ij}^{(1)}\right]-\bar{N}_{\theta\theta}\left[K_{ij}^{(3)}\right]\right)\{U\}=0, \qquad (12)$$

where $K_{ij}^{(k)}$ is the stiffness matrix. It should be noted that in the case of radial instability, only the outer tube (microtubule) is subjected to external pressure. In this case, the critical pressure is obtained as $P_{cr}=-\bar{N}_{\theta\theta}/R_m$ and the circumferential wave number is greater than or equal to two ($n_\theta\geq 2$) [32].

3. Results and discussion

To evaluate the precision of this modelling, the critical instability force of protein MTs subject to longitudinal compression is compared to that determined using optical trapping method [16]. Table 1 indicates the critical instability load of MTs stabilized with MAPs and taxol for different lengths. The calibrated values of size coefficients are also presented in

this table. It is assumed that the MT has 13 protofilaments and its geometric properties are considered as $R_m = 13$ nm, $h_m = 2.7$ nm and $h_{0m} = 1.6$ nm [32]. Since microtubules show strong anisotropic behavior, they are assumed to be orthotropic with four independent material constants. The longitudinal Young's moduli of MTs stabilized with MAPs and taxol are $E_x = 1 \, GPa$ and $E_x = 0.3 \, GPa$, respectively [16, 57]. For shear and circumferential moduli, we have $E_\theta/E_x = 0.001$ and $G_{x\theta}/E_x = 0.001$ [36]. A value of $v_x = 0.3$ is used for Poisson's ratio along longitudinal axes. From Table 1, it is observed that the presented modeling can be used to accurately describe the static instability of protein MTs. The calibrated values of e_0a for MTs stabilised with MAPs and taxol are determined as $e_0a = 10$ nm and $e_0a = 25$ nm, respectively. This implies that the nonlocal effects are more pronounced for taxol-stabilized MTs than MAP-stabilized MTs. In addition, the calibrated value of the strain gradient coefficient increases with increasing the length of the MT. It means that the strain gradient effects become more significant in the stability behavior of MTs as their length increases.

Table 1. Verification study for the static stability of MTs [16].

Samples	Length (μm)	Axial instability force (pN)		
		ℓ_s (nm)	Present	Experiment
MAP-stabilized MTs (10)[a]	10.5	18	3.0187	3.0
	19.9	27	1.5474	1.5
	27.9	39	1.4846	1.5
Taxol-stabilized MTs (25)[a]	4.4	7	0.7221	0.7
	11.8	25	0.3925	0.4

[a] The number in parentheses denotes the value of e_0a (nm).

The influence of taxol on the longitudinal instability load of the MT for different strain gradient parameters is demonstrated in Fig. 4. The material and geometric properties of the MAP-stabilized and taxol-stabilized microtubules are as stated above. The nonlocal parameter is taken as $e_0a = 10$ nm. The axial instability load reduces with increasing the length of the microtubule. The critical load of protein microtubules is greatly affected by taxol. The axial instability load of taxol-stabilized MTs is lower than that of MTs stabilised with MAPs. It implies that the stiffness of the MT decreases in the presence of taxol. Further, the critical axial force corresponding to static instability is higher for higher strain gradient coefficients for both types of microtubules. The effects of carbon nanotubes on the axial instability behavior of MTs for different values of size coefficients are indicated in Fig. 5. For CNTs, we have $E_ch_c = 360 \, J/m^2$, $v_c = 0.2$ and $D_c = 2$ eV [18]. The thickness of the CNT is 0.34 nm. It is assumed that before instability, the hybrid nanostructure is at the equilibrium state. The vdW coefficients related to the load exerting on the protein MT and CNT are $c_{vdW}^m = 29.246$ GPa/nm and $c_{vdW}^c = 40.011$ GPa/nm, respectively

[33, 58]. It is observed that CNTs have a prominent role in the instability response of microtubules. Unlike taxol, adding carbon nanotubes to cells increases the axial instability force of MTs. Further, the critical load decreases with the increase of nonlocal parameter. However, the strain gradient parameter has an increasing effect on the instability force.
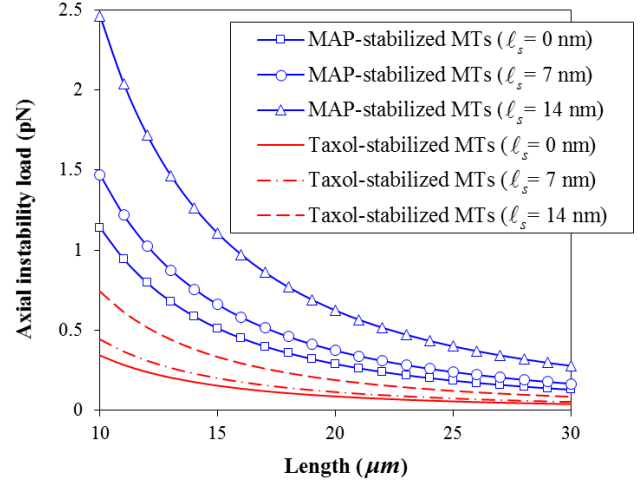
Fig. 4. Axial instability loads of protein MTs stabilised with MAPs and taxol versus length for different strain gradient coefficients.
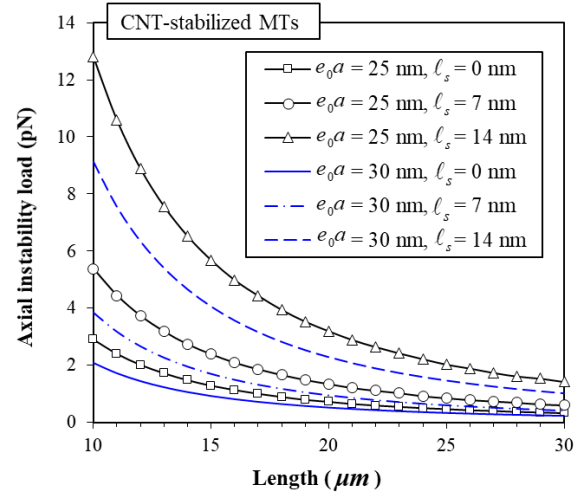
Fig. 5. Axial instability loads of protein MTs stabilised with MAPs and taxol versus length for different strain gradient and nonlocal coefficients.

To investigate the small scale effect on the radial instability of MTs stabilised with taxol and MAPs, the radial instability pressure versus the nonlocal coefficient is shown in Fig. 6 for various strain gradient coefficients. The length of the hybrid nanostructure is considered as $L = 10 \, \mu m$. The half axial wave number and the circumferential wave number are taken as $n_x = 1$ and $n_\theta = 2$, respectively. The CNT is assumed to be at the equilibrium distance from the MT prior to instability. The radial instability pressure gradually decreases as the nonlocal coefficient increases. Nonetheless, the instability pressure increases when strain gradient effects become stronger. The radial instability pressure of microtubules stabilized with taxol is smaller than those of MAP-stabilized microtubules. In addition, the role of strain gradients in the radial instability of MTs is

reduced by exposure of cells to taxol. Another interesting observation is that the effect of taxol becomes less significant for higher values of e_0a due to the strong nonlocality. Fig. 7 illustrates the change of radial instability pressure of protein MTs stabilized with both taxol and CNTs versus the nonlocal coefficient for different strain gradient coefficients. Comparing this figure to the previous one indicates that adding CNTs to cells leads to a substantial increase in the radial stability capacity of MTs. Furthermore, the strain gradient effect is less pronounced as the nonlocal coefficient increases.
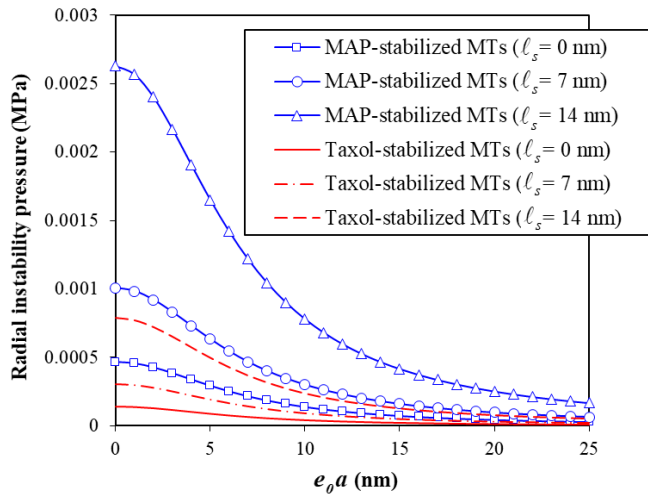
Fig. 6. Radial instability pressure of protein MTs stabilised with MAPs and taxol versus the nonlocal coefficient for various strain gradient coefficients.
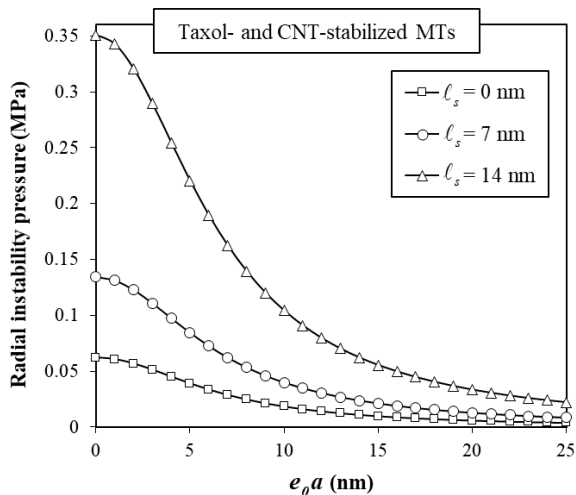
Fig. 7. Radial instability pressure of MTs stabilized with both taxol and CNTs versus the nonlocal coefficient for various strain gradient coefficients.

4. Conclusions

The static instability behavior of protein MTs stabilised with CNTs and taxol subject to radial and axial loads has been studied. Size-dependent modeling was performed applying a shell theory incorporating strain gradient and nonlocal influences. Exact solutions were presented for both radial instability pressure and axial instability loads of the hybrid nanostructure. Comparison of the results of the model for MAP- and taxol-stabilized MTs with the results of experiments reported in the literature indicated that

the present model with proper values of small scale parameters gives more precise results than the classical shell theory. It was found that stabilizing MTs with taxol reduces both the radial instability pressure and axial instability load of MTs. In addition, the nonlocal parameter has a decreasing effect on the stability capacity of CNT-stabilized MTs. However, the critical instability loads of the hybrid nanostructure increase with increasing the strain gradient effects. Unlike taxol, stabilizing MTs with CNTs leads to an increase in both axial instability force and radial instability pressure of MTs. Furthermore, for higher nonlocal coefficients, the influence of taxol becomes less pronounced.

References

[1] Z. Liu, S. Tabakman, K. Welsher, H. Dai, Carbon nanotubes in biology and medicine: in vitro and in vivo detection, imaging and drug delivery, *Nano research,* Vol. 2, No. 2, pp. 85-120, 2009.

[2] Z. Liu, W. Cai, L. He, N. Nakayama, K. Chen, X. Sun, X. Chen, H. Dai, In vivo biodistribution and highly efficient tumour targeting of carbon nanotubes in mice, *Nature nanotechnology,* Vol. 2, No. 1, pp. 47, 2007.

[3] P.-C. Lee, Y.-C. Chiou, J.-M. Wong, C.-L. Peng, M.-J. Shieh, Targeting colorectal cancer cells with single-walled carbon nanotubes conjugated to anticancer agent SN-38 and EGFR antibody, *Biomaterials,* Vol. 34, No. 34, pp. 8756-8765, 2013.

[4] S. Peretz, O. Regev, Carbon nanotubes as nanocarriers in medicine, *Current Opinion in Colloid & Interface Science,* Vol. 17, No. 6, pp. 360-368, 2012.

[5] N. M. Bardhan, D. Ghosh, A. M. Belcher, Carbon nanotubes as in vivo bacterial probes, *Nature communications,* Vol. 5, pp. 4918, 2014.

[6] A. Sharma, S. Hong, R. Singh, J. Jang, Single-walled carbon nanotube based transparent immunosensor for detection of a prostate cancer biomarker osteopontin, *Analytica chimica acta,* Vol. 869, pp. 68-73, 2015.

[7] L. García-Hevia, F. Fernández, C. Grávalos, A. García, J. C. Villegas, M. L. Fanarraga, Nanotube interactions with microtubules: implications for cancer medicine, *Nanomedicine,* Vol. 9, No. 10, pp. 1581-1588, 2014.

[8] L. Rodriguez-Fernandez, R. Valiente, J. Gonzalez, J. C. Villegas, M. n. L. Fanarraga, Multiwalled carbon nanotubes display microtubule biomimetic properties in vivo, enhancing microtubule assembly and stabilization, *ACS nano,* Vol. 6, No. 8, pp. 6614-6625, 2012.

[9] F. Gittes, B. Mickey, J. Nettleton, J. Howard, Flexural rigidity of microtubules and actin filaments measured from thermal fluctuations in shape, *The Journal of cell biology,* Vol. 120, No. 4, pp. 923-934, 1993.

[10] J. M. Berg, J. Tymoczko, L. Stryer, Glycolysis is an energy-conversion pathway in many organisms, *Biochemistry. 5th ed. New York: WH Freeman*, 2002.

[11] J. A. Kaltschmidt, A. H. Brand, Asymmetric cell division: microtubule dynamics and spindle asymmetry, *J Cell Sci,* Vol. 115, No. 11, pp. 2257-2264, 2002.

[12] H. Lodish, A. Berk, S. Zipursky, P. Matsudaira, D. Baltimore, J. Darnell, Collagen: the fibrous proteins of the matrix, *Molecular Cell Biology,* Vol. 4, 2000.

[13] K. Dastani, M. Moghimi Zand, A. Hadi, Dielectrophoretic effect of nonuniform electric fields on the protoplast cell, *Journal of Computational Applied Mechanics,* Vol. 48, No. 1, pp. 1-14, 2017.

[14] S. Suresh, Biomechanics and biophysics of cancer cells, *Acta Materialia,* Vol. 55, No. 12, pp. 3989-4014, 2007.

[15] F. Pampaloni, G. Lattanzi, A. Jonáš, T. Surrey, E. Frey, E.-L. Florin, Thermal fluctuations of grafted microtubules provide evidence of a length-dependent persistence length, *Proceedings of the National Academy of Sciences,* Vol. 103, No. 27, pp. 10248-10253, 2006.

[16] M. Kurachi, M. Hoshi, H. Tashiro, Buckling of a single microtubule by optical trapping forces: direct measurement of microtubule rigidity, *Cell motility and the cytoskeleton,* Vol. 30, No. 3, pp. 221-228, 1995.

[17] A. I. Aria, H. Biglari, Computational vibration and buckling analysis of microtubule bundles based on nonlocal strain gradient theory, *Applied Mathematics and Computation,* Vol. 321, pp. 313-332, 2018.

[18] Q. Wang, V. Varadan, Application of nonlocal elastic shell theory in wave propagation analysis of carbon nanotubes, *Smart Materials and Structures,* Vol. 16, No. 1, pp. 178, 2007.

[19] M. Ece, M. Aydogdu, Nonlocal elasticity effect on vibration of in-plane loaded double-walled carbon nano-tubes, *Acta Mechanica,* Vol. 190, No. 1-4, pp. 185-195, 2007.

[20] M. Danesh, A. Farajpour, M. Mohammadi, Axial vibration analysis of a tapered nanorod based on nonlocal elasticity theory and differential quadrature method, *Mechanics Research Communications,* Vol. 39, No. 1, pp. 23-27, 2012.

[21] M. Aydogdu, I. Elishakoff, On the vibration of nanorods restrained by a linear spring in-span, *Mechanics Research Communications,* Vol. 57, pp. 90-96, 2014.

[22] M. Z. Nejad, A. Hadi, A. Rastgoo, Buckling analysis of arbitrary two-directional functionally graded Euler–Bernoulli nano-beams based on nonlocal elasticity theory, *International Journal of Engineering Science,* Vol. 103, pp. 1-10, 2016.

[23] M. Z. Nejad, A. Hadi, Non-local analysis of free vibration of bi-directional functionally graded Euler–Bernoulli nano-beams, *International Journal of Engineering Science,* Vol. 105, pp. 1-11, 2016.

[24] A. Hadi, M. Z. Nejad, M. Hosseini, Vibrations of three-dimensionally graded nanobeams, *International Journal of Engineering Science,* Vol. 128, pp. 12-23, 2018.

[25] M. Z. Nejad, A. Hadi, A. Farajpour, Consistent couple-stress theory for free vibration analysis of Euler-Bernoulli nano-beams made of arbitrary bi-directional functionally graded materials, *Structural Engineering and Mechanics,* Vol. 63, No. 2, pp. 161-169, 2017.

[26] M. R. Farajpour, A. Shahidi, A. Farajpour, Resonant frequency tuning of nanobeams by piezoelectric nanowires under thermo-electro-magnetic field: a theoretical study, *Micro & Nano Letters,* Vol. 13, No. 11, pp. 1627-1632, 2018.

[27] A. Farajpour, M. Mohammadi, A. Shahidi, M. Mahzoon, Axisymmetric buckling of the circular graphene sheets with the nonlocal continuum plate model, *Physica E: Low-dimensional Systems and Nanostructures,* Vol. 43, No. 10, pp. 1820-1825, 2011.

[28] M. Farajpour, A. Shahidi, A. Hadi, A. Farajpour, Influence of initial edge displacement on the nonlinear vibration, electrical and magnetic instabilities of magneto-electro-elastic nanofilms, *Mechanics of Advanced Materials and Structures,* Vol. DOI: 10.1080/15376494.2018.1432820, 2018.

[29] M. Farajpour, A. Shahidi, A. Farajpour, A nonlocal continuum model for the biaxial buckling analysis of composite nanoplates with shape memory alloy nanowires, *Materials Research Express,* Vol. 5, No. 3, pp. 035026, 2018.

[30] M. R. Farajpour, A. R. Shahidi, A. Farajpour, Frequency behavior of ultrasmall sensors using vibrating SMA nanowire-reinforced sheets under a non-uniform biaxial preload, *Materials Research Express,* Vol. 6, pp. 065047, 2019.

[31] M. R. Farajpour, A. R. Shahidi, A. Farajpour, Frequency behavior of ultrasmall sensors using vibrating SMA nanowire-reinforced sheets under a non-uniform biaxial preload, *Materials Research Express,* Vol. 6, No. 6, pp. 065047, 2019/03/29, 2019.

[32] C. Wang, C. Ru, A. Mioduchowski, Orthotropic elastic shell model for buckling of microtubules, *Physical Review E,* Vol. 74, No. 5, pp. 052901, 2006.

[33] H. Jiang, L. Jiang, J. D. Posner, B. D. Vogt, Atomistic-based continuum constitutive relation for microtubules: elastic modulus prediction, *Computational Mechanics,* Vol. 42, No. 4, pp. 607-618, 2008.

[34] T. Li, A mechanics model of microtubule buckling in living cells, *Journal of biomechanics,* Vol. 41, No. 8, pp. 1722-1729, 2008.

[35] B. Akgöz, Ö. Civalek, Application of strain gradient elasticity theory for buckling analysis of protein microtubules, *Current Applied Physics,* Vol. 11, No. 5, pp. 1133-1138, 2011.

[36] M. Taj, J. Zhang, Analysis of wave propagation in orthotropic microtubules embedded within elastic medium by Pasternak model, *journal of the mechanical behavior of biomedical materials,* Vol. 30, pp. 300-305, 2014.

[37] A. Farajpour, A. Rastgoo, M. Mohammadi, Surface effects on the mechanical characteristics of microtubule networks in living cells, *Mechanics Research Communications,* Vol. 57, pp. 18-26, 2014.

[38] A. G. Arani, M. Abdollahian, M. Jalaei, Vibration of bioliquid-filled microtubules embedded in cytoplasm including surface effects using modified couple stress theory, *Journal of theoretical biology,* Vol. 367, pp. 29-38, 2015.

[39] Ö. Civalek, C. Demir, A simple mathematical model of microtubules surrounded by an elastic matrix by nonlocal finite element method, *Applied Mathematics and Computation,* Vol. 289, pp. 335-352, 2016.

[40] M. A. Jordan, L. Wilson, Microtubules as a target for anticancer drugs, *Nature Reviews Cancer,* Vol. 4, No. 4, pp. 253, 2004.

[41] C. Lim, G. Zhang, J. Reddy, A higher-order nonlocal elasticity and strain gradient theory and its applications in wave propagation, *Journal of the Mechanics and Physics of Solids,* Vol. 78, pp. 298-313, 2015.

[42] M. R. Farajpour, A. Rastgoo, A. Farajpour, M. Mohammadi, Vibration of piezoelectric nanofilm-based electromechanical sensors via higher-order non-local strain gradient theory, *Micro & Nano Letters,* Vol. 11, No. 6, pp. 302-307, 2016.

[43] L. Li, Y. Hu, L. Ling, Wave propagation in viscoelastic single-walled carbon nanotubes with surface effect under magnetic field based on nonlocal strain gradient theory, *Physica E: Low-dimensional Systems and Nanostructures,* Vol. 75, pp. 118-124, 2016.

[44] A. Farajpour, A. Rastgoo, M. Mohammadi, Vibration, buckling and smart control of microtubules using piezoelectric nanoshells under electric voltage in thermal environment, *Physica B: Condensed Matter,* Vol. 509, pp. 100-114, 2017.

[45] M. Mohammadi, A. Farajpour, M. Goodarzi, R. Heydarshenas, Levy type solution for nonlocal thermo-mechanical vibration of orthotropic mono-layer graphene sheet embedded in an elastic medium, *Journal of Solid Mechanics,* Vol. 5, No. 2, pp. 116-132, 2013.

[46] S. R. Asemi, A. Farajpour, Vibration characteristics of double-piezoelectric-nanoplate-systems, *IET Micro & Nano Letters,* Vol. 9, No. 4, pp. 280-285, 2014.

[47] S. R. Asemi, A. Farajpour, M. Borghei, A. H. Hassani, Thermal effects on the stability of circular graphene sheets via nonlocal continuum mechanics, *Latin American Journal of Solids and Structures,* Vol. 11, No. 4, pp. 704-724, 2014.

[48] M. Hosseini, A. Hadi, A. Malekshahi, M. Shishesaz, A review of size-dependent elasticity for nanostructures, *Journal of Computational Applied Mechanics,* Vol. 49, No. 1, pp. 197-211, 2018.

[49] N. Kordani, A. Fereidoon, M. Divsalar, A. Farajpour, Forced vibration of piezoelectric nanowires based on nonlocal elasticity theory, *Journal of Computational Applied Mechanics* Vol. 47, pp. 137-150, 2016.

[50] A. Farajpour, A. Rastgoo, M. Farajpour, Nonlinear buckling analysis of magneto-electro-elastic CNT-MT hybrid nanoshells based on the nonlocal continuum mechanics, *Composite Structures,* Vol. 180, pp. 179-191, 2017.

[51] M. Goodarzi, M. Mohammadi, A. Farajpour, M. Khooran, Investigation of the effect of pre-stressed on vibration frequency of rectangular nanoplate based on a visco-Pasternak foundation, *Journal of Solid Mechanics,* Vol. 6, pp. 98-121, 2014.

[52] S. R. Asemi, M. Mohammadi, A. Farajpour, A study on the nonlinear stability of orthotropic single-layered graphene sheet based on nonlocal elasticity theory, *Latin American Journal of Solids and Structures,* Vol. 11, No. 9, pp. 1515-1540, 2014.

[53] M. Mohammadi, A. Farajpour, M. Goodarzi, H. Mohammadi, Temperature effect on vibration analysis of annular graphene sheet embedded on visco-Pasternak foundation, *Journal of Solid Mechanics,* Vol. 5, No. 3, pp. 305-323, 2013.

[54] A. Farajpour, A. Rastgoo, Influence of carbon nanotubes on the buckling of microtubule bundles in viscoelastic cytoplasm using nonlocal strain gradient theory, *Results in physics,* Vol. 7, pp. 1367-1375, 2017.

[55] M. Farajpour, A. Shahidi, F. Tabataba'i-Nasab, A. Farajpour, Vibration of initially stressed carbon nanotubes under magneto-thermal environment for nanoparticle delivery via higher-order nonlocal strain gradient theory, *The European Physical Journal Plus,* Vol. 133, No. 6, pp. 219, 2018.

[56] A. C. Eringen, 2002, *Nonlocal continuum field theories*, Springer Science & Business Media,

[57] C. Li, C. Ru, A. Mioduchowski, Length-dependence of flexural rigidity as a result of anisotropic elastic properties of microtubules, *Biochemical and biophysical research communications,* Vol. 349, No. 3, pp. 1145-1150, 2006.

[58] W. D. Cornell, P. Cieplak, C. I. Bayly, I. R. Gould, K. M. Merz, D. M. Ferguson, D. C. Spellmeyer, T. Fox, J. W. Caldwell, P. A. Kollman, A second generation force field for the simulation of proteins, nucleic acids, and organic molecules, *Journal of the American Chemical Society,* Vol. 117, No. 19, pp. 5179-5197, 1995.